Depth-optimized quantum circuit synthesis for diagonal unitary operators with asymptotically optimal gate count

Shihao Zhang [1,2] Kai Huang,[1] and Lvzhou Li [1,*]

[1]*School of Computer Science and Engineering, Sun Yat-sen University, Guangzhou 510006, China*

[2]*Hebei Provincial Key Laboratory of Photoelectric Control on Surface and Interface, School of Science, Hebei University of Science and Technology, Shijiazhuang 050018, China*

(Received 7 October 2023; accepted 29 February 2024; published 1 April 2024)

Diagonal unitary operators are well known to be key building blocks of many quantum algorithms and quantum computing procedures, and thus resource-efficient quantum circuit implementations are in demand. Here we propose a constructive algorithm that can generate a quantum circuit over the primitive gate set {CNOT, R_Z} for realizing any given diagonal unitary operator piece by piece. The theoretical analysis reveals that, for the general case, our generated circuit not only ensures the asymptotically optimal gate count, but also nearly halves the circuit depth compared with the previous Welch's method [New J. Phys. **16**, 033040 (2014)]. Specifically, this substantial depth optimization originates from the use of a uniform circuit rewriting rule developed here. The performance of our circuit synthesis algorithm is further validated by numerical evaluations on two examples. First, we achieve a nearly 50% depth reduction over Welch's method for synthesizing random diagonal unitary operators with up to 16 qubits. Second, we achieve an average of 22.05% depth reduction for resynthesizing the diagonal part of the specific quantum approximate optimization algorithm (QAOA) circuits with up to 14 qubits.

DOI: 10.1103/PhysRevA.109.042601

I. INTRODUCTION

Translating a high-level quantum operation into a gate-based quantum circuit, usually called *quantum circuit synthesis*, forms one of the theoretical foundations of quantum computing and has been intensively studied since the 1990s [1–11]. While the number of elementary gates for realizing arbitrary unitaries scales with $O(4^n)$ [4,6], in some situations we are more interested in the efficient synthesis of a specific kind of quantum operator rather than general unitary matrices, e.g., the diagonal unitary operator that can add different phase factors to distinct computational basis states. Diagonal operators and their associated circuits are revealed to have nontrivial computational power and applications in quantum computing [12], e.g., as important parts in Grover search [13–15], quantum approximate optimization algorithm (QAOA) [16,17], quantum algorithms for string problems [18,19], quantum simulation [20–22], and the generation of a t-design of random states [23]. Therefore, the synthesis of low-cost quantum circuits for implementing diagonal unitary operators is critical for executing a variety of quantum computing tasks. In general, the gate count and circuit depth of the synthesized circuits are expected to be minimized to reduce the impact of gate errors and decoherence in realistic devices [16,24].

Over the years, methods to construct quantum circuits over the two-qubit controlled-NOT gate (CNOT) and single-qubit Z-axis rotation gate $R_Z(\theta)$ for implementing diagonal unitary operators with the asymptotically optimal gate count have been proposed [20,25]. More specifically, given an n-qubit diagonal unitary operator, a quantum circuit over the gate set {CNOT, R_Z} can be constructed with a total of $2^{n+1}-3$ gates in the worst case, including 2^n-2 CNOT gates and 2^n-1 R_Z gates. However, these works have not discussed whether the depth of the synthesized circuit can be further reduced. As is well known, depth-optimized circuits are important to a robust implementation of a quantum algorithm on near-term quantum hardware since a shorter depth corresponds to shorter circuit execution time as well as a reduction of errors due to decoherence [24,26]. In this paper, we aim at algorithms that produce the quantum circuit over the gate set {CNOT, R_Z} for any given diagonal unitary operator, with a particular focus on reducing the circuit depth, while keeping the asymptotically optimal gate count. Our contributions are summarized as follows.

(1) We derive a procedure to construct the quantum {CNOT, R_Z} circuit for implementing a general n-qubit diagonal unitary operator with the asymptotically optimal gate count $2^{n+1}-3$ (Theorem 1), and then develop a uniform circuit rewriting rule (Theorem 2) that is well suited for optimizing the depth of such circuits.

(2) By observing the structure of the resultant circuits in (1), we further propose a self-contained depth-optimized circuit synthesis algorithm (Algorithm 1) that not only ensures the asymptotically optimal gate count $2^{n+1}-3$, but also provides a nearly half reduction in circuit depth over Welch's method [20] for the general case of large size.

(3) Finally, the practical performance of our synthesis algorithm is evaluated on two typical cases. First, we synthesize

*lilvzh@mail.sysu.edu.cn

the general random diagonal unitary operator with up to 16 qubits and achieve a nearly 50% depth reduction compared with Welch's method. Second, we resynthesize the diagonal part of specific QAOA circuits with up to 14 qubits and achieve an average of 22.05% depth reduction.

The rest of this paper is organized as follows. Section II introduces some useful notations and facts about quantum circuit design. Section III proposes a depth-optimized synthesis algorithm for generating quantum circuits over {CNOT, R_Z} gates that can implement arbitrary diagonal unitary operators with both the asymptotically optimal gate count and an optimized depth for the general case. Section IV performs evaluations on two typical instances to illustrate the performance of our circuit synthesis algorithm. Section V concludes the paper.

II. PRELIMINARIES

For the reader's convenience, in this section we introduce some basic notations and facts about the quantum circuit model and synthesis algorithm throughout the paper.

A. Notations

We denote the integer set $\{a, a+1, a+2, \ldots, b\}$ by $[a, b]$ with $a \leqslant b$. A t-bit string with all 0 (or 1) is denoted as $0^{(t)}$ (or $1^{(t)}$). For each string $j = j_1 j_2 \ldots j_n$, we denote the set of indices of all "1" bits as $P_j = \{p_1, p_2, \ldots, p_m\}$ such that $j_{p_1} = j_{p_2} = \cdots = j_{p_m} = 1$ with m being the Hamming weight of j. The symbol $\circ$ is used to concatenate $m (m \geqslant 2)$ subcircuits $\{QC_1, QC_2, \ldots, QC_m\}$ to form a circuit QC such that $QC = QC_1 \circ QC_2 \circ \ldots \circ QC_m$. The commonly used identity and Hadamard matrices are

$$I = \begin{pmatrix} 1 & 0 \\ 0 & 1 \end{pmatrix}, \quad H = \frac{1}{\sqrt{2}} \begin{pmatrix} 1 & 1 \\ 1 & -1 \end{pmatrix}. \tag{1}$$

B. Quantum circuits over {CNOT, R_Z} gates

The CNOT gate and Z-basis rotation gate (R_Z), respectively, act on the two- and one-qubit basis state as follows:

$$\text{CNOT}(c, t)|k_c\rangle|k_t\rangle = |k_c\rangle|k_t \oplus k_c\rangle, \tag{2}$$

$$R_Z(-\beta; r)|k_r\rangle = \begin{pmatrix} e^{i\beta/2} & 0 \\ 0 & e^{-i\beta/2} \end{pmatrix} |k_r\rangle = e^{i\beta(-1)^{k_r}/2}|k_r\rangle, \tag{3}$$

for any qubits $c, t, r \in [1, n]$. The indices c and t in CNOT(c, t) denote the control and target qubit it acts on, respectively. The single-qubit gate $R_Z(-\beta; r)$ acts on qubit r with a rotation angle $\beta \in [0, 2\pi)$. A simple {CNOT, R_Z} circuit example is shown in Fig. 1, which consists of two CNOT gates denoted CNOT(1,2,1) and CNOT(2,4,2) as well as three R_Z gates denoted $R_Z(-\beta_1; 3, 1)$, $R_Z(-\beta_2; 2, 3)$, and $R_Z(-\beta_3; 4, 3)$ indicated by gray squares. Note the third parameter of the CNOT or R_Z gate indicates its column index in the circuit.

In the following, we introduce some commutation and rewriting rules that will be used to achieve our substantial depth-optimization goal in Sec. III C.

Commutation rules for CNOT *gates.* From the basis transformation about a CNOT gate in Eq. (2), it can be verified that CNOT(c_2, t_2) commutes with CNOT(c_1, t_1) only when both $c_2 \neq t_1$ and $c_1 \neq t_2$ are satisfied. Another useful commutation relation presented in Fig. 2(a) can be used to reduce three CNOT gates to two.

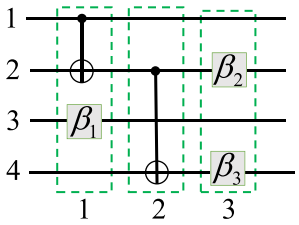

FIG. 1. A simple four-qubit and three-depth circuit consisting of two CNOT gates denoted CNOT(1,2,1) and CNOT(2,4,2) as well as three R_Z gates denoted $R_Z(-\beta_1; 3, 1)$, $R_Z(-\beta_2; 2, 3)$, and $R_Z(-\beta_3; 4, 3)$, respectively.

Commutation rules for R_Z *gates.* Obviously, any two $R_Z(-\beta)$ gates commute with each other and can be directly merged into a new one according to Eq. (3).

Commutation rules for R_Z *and* CNOT *gates.* $R_Z(-\beta; c)$ gate commutes with CNOT(c, t) as shown in Fig. 2(b).

Rewriting rules for {CNOT, R_Z} *subcircuits.* Rewriting rules indicate broader commutation relations between subcircuits over {CNOT, R_Z} [27]. For example, the combination of rules in Figs. 2(a) and 2(b) can lead to a result in Fig. 2(c) where CNOT(c, t) $\circ$ $R_Z(-\beta; t)$ $\circ$ CNOT(c, t) commutes with CNOT(t, $r \neq c$) as well as an extended result in Fig. 2(d). Note the subcircuit in the red dashed box of Figs. 2(c) and 2(d) can be generalized to the case that consists of an even number of CNOT(c_i, t) for each control qubit c_i together with any number of $R_Z(-\beta; t)$.

C. Quantum circuit synthesis algorithm

A quantum circuit synthesis algorithm is an algorithm that can synthesize a quantum circuit over a certain gate set for realizing the target unitary operator, and the gate count and circuit depth are two important cost metrics in circuit synthesis. A quantum circuit can be represented as a directed acyclic graph (DAG) in which each node corresponds to the circuit's gate and each edge corresponds to the input or output of a gate.

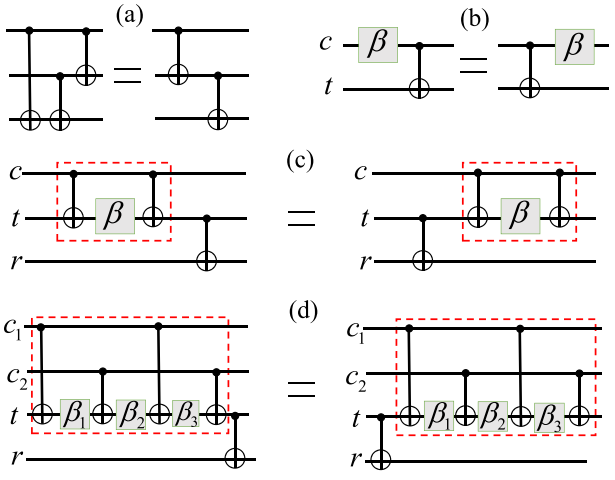

FIG. 2. Some useful commutation and rewriting rules for {CNOT, R_Z} circuits.

Then the circuit depth d is defined as the maximum length of a path flowing from an input of the circuit to an output [7]. Equivalently speaking, d is the number of layers of quantum gates that compactly act on all disjoint sets of qubits [26,28], and thus a smaller d indicates a shorter execution time of a circuit. In general, a circuit synthesis algorithm can have different circuit complexities for implementing different input unitary operators, and the upper bound among all cases is called the worst-case behavior of this algorithm and usually used to evaluate the algorithm's performance.

III. DEPTH-OPTIMIZED SYNTHESIS OF CIRCUITS FOR DIAGONAL UNITARY OPERATORS

For realizing general diagonal unitary operators, in this section we first derive a procedure that directly starts from matrix decomposition to quantum circuit construction with an asymptotically optimal gate count over $\{\text{CNOT}, R_Z\}$ (summarized as Theorem 1), and then propose a uniform circuit rewriting rule well suited for circuit depth optimization (see Theorem 2). Based on these results, we make a further step towards a straightforward depth-optimized synthesis algorithm (Algorithm 1) that can automatically achieve a nearly 50% reduction in circuit depth compared with Ref. [20] for implementing large-size operators. In addition to the general case, we also discuss the possible optimization on special cases.

A. Matrix decomposition

For a general size $N \times N$ ($N = 2^n$) diagonal unitary operator in matrix form

$$D(\overrightarrow{\theta}) = \begin{bmatrix} e^{i\theta_{00..00}} & 0 & 0 & 0 \\ 0 & e^{i\theta_{00..01}} & 0 & 0 \\ \vdots & \vdots & \ddots & \vdots \\ 0 & 0 & 0 & e^{i\theta_{11..11}} \end{bmatrix}, \tag{4}$$

its angle parameters $\overrightarrow{\theta} = [\theta_{00..00}, \theta_{00..01}, \ldots, \theta_{11..11}]^T$ can be expanded by another set of parameters $\overrightarrow{\alpha} = [\alpha_{00..00}, \alpha_{00..01}, \ldots, \alpha_{11..11}]^T$ through the n-qubit Hadamard transform as

$$\overrightarrow{\theta} = \widetilde{H}\overrightarrow{\alpha}, \tag{5}$$

with $\widetilde{H} = H^{\otimes n} = \widetilde{H}^{\dagger}$ and H in Eq. (1). The effect of $\widetilde{H}$ on a basis state $|j\rangle$ is

$$\widetilde{H}|j\rangle = \frac{1}{\sqrt{2^n}} \sum_{k\in\{0,1\}^n} (-1)^{j\cdot k}|k\rangle, \tag{6}$$

with $j \cdot k = j_1k_1 \oplus j_2k_2 \oplus \cdots \oplus j_nk_n$ for $j = j_1j_2 \ldots j_n$ and $k = k_1k_2 \ldots k_n$. The element of $\widetilde{H}$ is given by $\widetilde{H}_{j,k} = \widetilde{H}_{k,j} = \langle k|\widetilde{H}|j\rangle = (-1)^{j\cdot k}\frac{1}{\sqrt{2^n}}$. Therefore, $\overrightarrow{\alpha}$ can be solved from the given $\overrightarrow{\theta}$ as

$$\overrightarrow{\alpha} = \widetilde{H}\overrightarrow{\theta}, \tag{7}$$

with

$$\alpha_j = \sum_{k\in\{0,1\}^n} \widetilde{H}_{j,k}\theta_k = \frac{1}{\sqrt{2^n}} \sum_{k\in\{0,1\}^n} (-1)^{j\cdot k}\theta_k. \tag{8}$$

By inserting Eq. (5) into Eq. (4), the matrix $D(\overrightarrow{\theta})$ can be decomposed into a product of N commutative diagonal matrices $B_j(\alpha_j)$ as

$$D(\overrightarrow{\theta}) = \prod_{j\in\{0,1\}^n} B_j(\alpha_j), \tag{9}$$

where the diagonal element indexed by $k \in \{0, 1\}^n$ of $B_j(\alpha_j)$ is

$$B_j^{(k)}(\alpha_j) = \exp[i\widetilde{H}_{k,j}\alpha_j] = \exp\left[\frac{i\alpha_j}{\sqrt{2^n}}(-1)^{j\cdot k}\right]. \tag{10}$$

Therefore, the effect of $B_j(\alpha_j)$ on an n-qubit computational basis state $|k\rangle$ is to apply a phase shift as

$$B_j(\alpha_j)|k\rangle = \exp\left[\frac{i\alpha_j}{\sqrt{2^n}}(-1)^{j\cdot k}\right]|k\rangle. \tag{11}$$

Using $P_j = \{p_1, p_2, \ldots, p_m\}$ associated with the string j as defined in Sec. II A, Eq. (11) can be written as

$$\begin{aligned} &B_j(\alpha_j)|k_1\rangle|k_2\rangle \cdots |k_n\rangle \\ &\quad = \exp\left[\frac{i\alpha_j}{\sqrt{2^n}}(-1)^{k_{p_1}\oplus k_{p_2}\oplus\cdots\oplus k_{p_m}}\right]|k_1\rangle|k_2\rangle \cdots |k_n\rangle, \end{aligned} \tag{12}$$

where the added phase factor of the basis state $|k\rangle = |k_1\rangle|k_2\rangle \cdots |k_n\rangle$ is uniquely determined by j and k.

B. Gate-count optimal circuit construction

For implementing the target diagonal operator in Eq. (4), we consider constructing a $\{\text{CNOT}, R_Z\}$ circuit module M_j to perform each matrix $B_j(\alpha_j)$ described in Eq. (12) in three steps: (i) apply $(m-1)$ CNOT gates denoted by $\text{CNOT}(p_1, p_m)$, $\text{CNOT}(p_2, p_m)$,..., $\text{CNOT}(p_{m-1}, p_m)$, respectively; (ii) apply a $R_Z(-\beta_j; p_m)$ gate in Eq. (3) with

$$\beta_j = \alpha_j/\sqrt{2^{n-2}} \tag{13}$$

and α_j given in Eq. (8); (iii) apply $(m-1)$ CNOT gates denoted by $\text{CNOT}(p_{m-1}, p_m)$, $\text{CNOT}(p_{m-2}, p_m)$, …, $\text{CNOT}(p_1, p_m)$, respectively.

According to Eqs. (2) and (3), such a constructed module M_j acts on any input basis state $|k_1\rangle|k_2\rangle \ldots |k_n\rangle$ as

$$\begin{aligned} &|k_1\rangle|k_2\rangle \ldots |k_{p_m}\rangle \ldots |k_n\rangle \\ &\xrightarrow{\text{(i)}} |k_1\rangle|k_2\rangle \ldots \left|\bigoplus_{i=1}^{m} k_{p_i}\right\rangle \ldots |k_n\rangle \\ &\xrightarrow{\text{(ii)}} \exp\left[\frac{i\alpha_j}{\sqrt{2^n}}(-1)^{k_{p_1}\oplus k_{p_2}\oplus\ldots\oplus k_{p_m}}\right]|k_1\rangle \ldots \left|\bigoplus_{i=1}^{m} k_{p_i}\right\rangle \ldots |k_n\rangle \\ &\xrightarrow{\text{(iii)}} \exp\left[\frac{i\alpha_j}{\sqrt{2^n}}(-1)^{k_{p_1}\oplus k_{p_2}\oplus\ldots\oplus k_{p_m}}\right]|k_1\rangle \ldots |k_{p_m}\rangle \ldots |k_n\rangle, \end{aligned} \tag{14}$$

which thus exactly performs $B_j(\alpha_j)$ described in Eq. (12).

Note the matrix $B_j(\alpha_j)$ and its associated circuit module M_j have the following features.

(1) For $j = 0^{(n)}$, Eq. (10) shows $B_0(\alpha_0) = e^{i\alpha_0/\sqrt{2^n}}I$ is just an identity matrix.

(2) For j including only one "1" such that $P_j = \{p_1\}$, M_j only consists of a single-qubit gate $R_Z(-\alpha_j/\sqrt{2^{n-2}}; p_1)$.

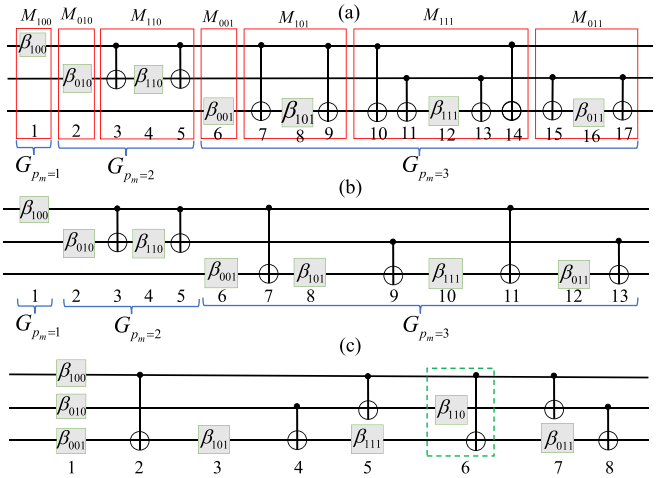

FIG. 3. An example with $n = 3$ qubits to demonstrate circuit construction and optimization as described in Sec. III B. (a) {CNOT, R_Z} circuit $QC_D = G_{p_m=1} \circ G_{p_m=2} \circ G_{p_m=3}$ consisting of $2^n - 1 = 7$ R_Z gates and $n2^n - 2^{n+1} + 2 = 10$ CNOT gates with total depth 15. (b) Circuit consisting of $2^n - 1 = 7$ R_Z gates and $2^n - 2 = 6$ CNOT gates with depth 11 after CNOT-count optimization of (a), which can be transformed into (c) with a shorter depth 8.

(3) The N diagonal matrices $B_j(\alpha_j)$ can be arranged in any order for realizing the target $D(\overrightarrow{\theta})$ due to their commutativity, i.e., Eq. (9) can be written as

$$D(\overrightarrow{\theta}) = B_{s_1}(\alpha_{s_1}) \dots B_{s_{N-1}}(\alpha_{s_{N-1}}), \tag{15}$$

where the trivial identity matrix $B_0(\alpha_0)$ is omitted and $\{s_1, s_2, \dots, s_{N-1}\}$ is an arbitrary permutation of $\{00\dots01, 00\dots10, \dots, 11\dots11\}$. Accordingly, the order of all nontrivial circuit modules $\{M_j : j \in \{0,1\}^n \backslash 0^{(n)}\}$ in the entire quantum circuit QC_D for realizing D can be exchanged at will.

In the following, we first specify the whole circuit QC_D by dividing all constituent modules M_j into n different groups, and then optimize each group by a technique from binary Gray codes to reduce the CNOT gate count.

We categorize a total of $(N-1)$ modules M_j into n groups denoted by $G_{p_m=1}, \dots, G_{p_m=n}$, where the integer $p_m \in [1, n]$ specifies the index of the rightmost "1" bit in $j = j_1 j_2 \dots j_n$. According to our circuit module construction above Eq. (14), each M_j in the group G_{p_m} applies a $R_Z(-\beta; p_m)$ gate as well as $2(m-1)$ CNOT gates between the control qubits $\{p_1, p_2, \dots, p_{m-1}\}$ and the target qubit p_m. As a consequence, each M_j in a given G_{p_m} can be uniquely represented by a $(p_m - 1)$-bit string $j_{1\to p_m-1} = j_1 j_2 \dots j_{p_m-1}$ such that the index of each "1" bit in $j_{1\to p_m-1}$ indicates the control qubit of each CNOT gate in M_j. In this view, each group G_{p_m} totally has $\sum_{m=1}^{p_m} C_{p_m-1}^{m-1} = 2^{p_m-1}$ such M_j and $2\sum_{m=1}^{p_m}(m-1)C_{p_m-1}^{m-1} = (p_m-1)2^{p_m-1}$ CNOT gates by simple counting principles, and thus $QC_D = G_{p_m=1} \circ G_{p_m=2} \circ \dots \circ G_{p_m=n}$ includes $\sum_{p_m=1}^{n} 2^{p_m-1} = 2^n - 1$ R_Z gates and $\sum_{p_m=1}^{n}(p_m-1)2^{p_m-1} = n2^n - 2^{n+1} + 2$ CNOT gates. The example with $n = 3$ qubits for the circuit QC_D constructed in this way is presented in Fig. 3(a).

Next, since all modules M_j in each G_{p_m} commute, here we can explore the reduction in CNOT gate count by making use of GRAY codes [29,30]. As shown in the transformation from Figs. 3(a) to 3(b), when two adjacent modules M_j and $M_{j'}$ in a G_{p_m} lead to only one "1" bit in the resultant string $j_{1\to p_m-1} \oplus j'_{1\to p_m-1}$, all but one CNOT gates will cancel between any two consecutive R_Z gates in M_j and $M_{j'}$. Based on this observation, we can arrange each G_{p_m} as a sequence of modules M_j with j, respectively, taken as

$$j = g_1 10^{(n-p_m)}, g_2 10^{(n-p_m)}, \dots, g_t 10^{(n-p_m)}, \tag{16}$$

and $t = 2^{p_m-1}$. Here $\{g_1, g_2, \dots, g_t\} = GC_t$ is a (p_m-1)-bit reflected GRAY code sequence which can be constructed iteratively for each p_m as

$$p_m = 2 : GC_t = \{0, 1\}, \tag{17a}$$

$$p_m \geqslant 3 : GC_t = \{GC_{t/2}\{0\}, \overline{GC_{t/2}}\{1\}\}, \tag{17b}$$

where $\overline{GC_{t/2}}$ is the reverse string sequence of $GC_{t/2}$, and $GC_{t/2}\{0\}$ or $\overline{GC_{t/2}}\{1\}$ indicates adding a suffix "0" or "1" to each string in $GC_{t/2}$ or $\overline{GC_{t/2}}$. This GRAY code sequence for each p_m would lead to only one CNOT gate located between any two consecutive R_Z gates in G_{p_m}. More specifically, all these 2^{p_m-1} CNOT gates in each G_{p_m} are targeted on qubit p_m, and from Eq. (17) we can iteratively identify the set of their control qubits denoted by $\lambda_{p_m}(p_m \geqslant 2)$ as

$$p_m = 2 : \lambda_2 = [1, 1], \tag{18}$$

and

$$p_m \geqslant 3 : \lambda_{k-1}(2^{k-2}) \leftarrow k-1, \lambda_k \leftarrow [\lambda_{k-1}, \lambda_{k-1}], \tag{19}$$

with k increasing from 3 to p_m.

In this way, the group $G_{p_m=1}$ contains one R_Z gate while each group $G_{p_m\geqslant 2}$ contains 2^{p_m-1} R_Z gates and 2^{p_m-1} CNOT gates after CNOT cancellation. As a result, our whole quantum circuit $QC_D = G_{p_m=1} \circ G_{p_m=2} \circ \dots \circ G_{p_m=n}$ contains $1 + \sum_{p_m=2}^{n} 2^{p_m-1} = 2^n - 1$ R_Z gates and $\sum_{p_m=2}^{n} 2^{p_m-1} = 2^n - 2$CNOT gates with the total number of gates being $2^{n+1} - 3$. Note that this total gate count has been proved to be asymptotically optimal for implementing n-qubit diagonal unitary matrices in the worst case [25]. For convenience, we summarize the above circuit construction procedure as Theorem 1, with an instance circuit for $n = 3$ shown in Fig. 3(b).

Theorem 1. Asymptotically gate-count optimal circuit construction. An n-qubit {CNOT, R_Z} quantum circuit QC_D for implementing a given operator $D(\overrightarrow{\theta})$ in Eq. (4) can be constructed as a sequence of n groups $QC_D = G_{p_m=1} \circ G_{p_m=2} \circ \dots \circ G_{p_m=n}$, where $G_{p_m=1}$ is a $R_Z(-\beta_{10^{(n-1)}}; 1)$ gate and each $G_{p_m\geqslant 2}$ consists of an alternating sequence of 2^{p_m-1} R_Z gates acting on qubit p_m and 2^{p_m-1} CNOT gates with their targets being p_m. More precisely, in each $G_{p_m\geqslant 1}$ the angle parameters β_j of these $R_Z(-\beta_j; p_m)$ gates can be solved by first determining 2^{p_m-1} different indices j according to Eqs. (16) and (17) and then using Eqs. (13) and (8), while all CNOT gate controls in each $G_{p_m\geqslant 2}$ can be determined by using Eqs. (18) and (19). The total gate count of such QC_D is asymptotically optimal as $2^{n+1} - 3$.

In addition to the gate count of the generated circuit, it is worth considering the circuit depth as another important circuit cost metric. For example, our constructed circuit in Fig. 3(b) has depth 11 for $n = 3$, which is shorter than Welch's three-qubit circuit of depth 13 (see Fig. 5 of Ref. [20]). The reason for this advantage is that our construction introduced above actually adopts a different Gray code sequence [see Eq. (17)] from Welch's for reducing the number of CNOT gates in each G_{p_m}, which naturally enables the parallelization of certain gates in two adjacent G_{p_m}. Furthermore, note that such circuits can be further optimized in terms of depth by considering appropriate circuit rewriting rules, e.g., the circuit of depth 11 in Fig. 3(b) can be transformed into one of depth 8 as shown in Fig. 3(c) by using the rule in Fig. 2(c). In the following, we investigate how to significantly reduce the depth of an n-qubit circuit obtained from Theorem 1 by further parallelizing its constituent gates and subcircuits, and finally derive a direct depth-optimized circuit synthesis algorithm in Sec. III C.

C. Depth-optimized synthesis algorithm

Step by step, in this section we first describe how to put forward a uniform circuit rewriting rule in Theorem 2 to significantly reduce the depth of the synthesized {CNOT, R_Z} circuit QC_D in Theorem 1, and then further derive a self-contained synthesis algorithm denoted Algorithm 1 that can directly produce a depth-optimized circuit for realizing target $D(\vec{\theta})$.

Intuitively, the movements of R_Z and CNOT gates or subcircuits within their located rows to fill vacancies of the original circuit by following certain rules are likely to cause a reduction in circuit depth, such as from Figs. 3(b) to 3(c). In this three-qubit circuit example, we move the subpart CNOT $\circ$ $R_Z(-\beta_{110})\circ$ CNOT in columns 3 to 5 of Fig. 3(b) to the right to fill the vacancies in columns 10 to 12 according to the rules in Fig. 2(c) and then parallelize $R_Z(-\beta_{100})$, $R_Z(-\beta_{010})$, and $R_Z(-\beta_{001})$ into one column, leading to a depth reduction from 11 to 8 as shown in Fig. 3(c). A more general instance to illustrate such depth-optimization procedure is provided in Fig. 4, where we present the four-qubit circuit constructed by Theorem 1 that consists of four subcircuits $G_{p_m=1,2,3,4}$ with total depth 24. For convenience, each gate is indexed by its row (1 to 4) and column (1 to 29) number before depth-optimization, and then we declare the subcircuits $G_{p_m=1}$, $G_{p_m=2}$, and $G_{p_m=3}$ can all be moved and embedded into appropriate vacancies of $G_{p_m=4}$ by the following steps.

(1) Move the subcircuit inside the red solid line box in columns 7 to 13 of $G_{p_m=3}$ to the right, which can commute with the CNOT gate in column 21 according to Fig. 2(d) and then fill the vacancies in columns 22 to 28 of $G_{p_m=4}$.

(2) Move the gate $R_Z(-\beta_{0010})$ inside the purple solid line box in column 6 of $G_{p_m=3}$ to the vacant position at row 3 and column 14 of $G_{p_m=4}$.

(3) Move the subcircuit inside the blue solid line box in columns 3 to 5 of $G_{p_m=2}$ to the right, which can commute with the CNOT gate in column 17 according to Fig. 2(c) and then fill the vacancies in columns 18 to 20 of $G_{p_m=4}$.

ALGORITHM 1. Depth-Optimized {CNOT, R_Z} Circuit Synthesis for implementing $D(\vec{\theta})$.

Input: A target diagonal operator $D(\vec{\theta})$ in Eq. (4).
Output: A depth-optimized {CNOT,R_Z} circuit QC_D for realizing $D(\vec{\theta})$.

Calculate all $2^n - 1$ rotation angles β_j using Eqs. (13) and (8), $QC_D \leftarrow$ Vacancy$(n, 2^n)$, $\lambda \leftarrow [0]$, $GC_2 \leftarrow \{0, 1\}$;
for $r = 1$ **to** $n - 1$ **do** // Embed $n - 1$ R_Z gates in column 1 of QC_D at first.
  Embed $R_Z(-\beta_{0^{(r-1)}10^{(n-r)}})$ in $QC_D(r, 1)$;
end
for $p_m = 2$ **to** n **do**
  $t \leftarrow 2^{p_m-1}$;
  $\lambda(t/2) \leftarrow p_m - 1$;
  $\lambda \leftarrow [\lambda, \lambda]$; // Identify all CNOT gate controls in $S_{p_m>1}$.
  if $p_m < n$ **then** // Identify and Embed gates of $S_{p_m<n}$ defined in Theorem 2.
    Embed a CNOT in $QC_D(1, p_m, 2^{p_m} + 1)$;
    for $i = 2$ **to** t **do**
      $j \leftarrow GC_t(i)10^{(n-p_m)}$;
      Embed $R_Z(-\beta_j)$ in $QC_D(p_m, 2^{p_m} + 2i - 2)$;
      Embed a CNOT in $QC_D(\lambda(i), p_m, 2^{p_m} + 2i - 1)$;
    end
    // Generate Gray code sequence.
    $GC_{2t} \leftarrow \{GC_t\{0\}, \overline{GC_t}\{1\}\}$; // $\overline{GC_t}$:reverse string sequence of GC_t.
  end
end
for $i = 1$ **to** 2^{n-1} **do** // Identify and Embed gates of $G_{p_m=n}$ finally.
  $j \leftarrow GC_{2^{n-1}}(i)1$;
  Embed $R_Z(-\beta_j)$ in $QC_D(n, 2i - 1)$;
  Embed a CNOT in $QC_D(\lambda(i), n, 2i)$;
end
return QC_D.

(4) Move the gate $R_Z(-\beta_{0100})$ inside the orange solid line box in column 2 of $G_{p_m=2}$ to the vacant position at row 2 and column 14 of $G_{p_m=4}$.

(5) Move the gate $R_Z(-\beta_{1000})$ inside the green solid line box in column 1 of $G_{p_m=1}$ to the vacant position at row 1 and column 14 of $G_{p_m=4}$.

As a result, the depth of such optimized 4-qubit circuit is the same as that of $G_{p_m=4}$ and equal to 16.

In above steps (1) and (3), the use of rewriting rules in Figs. 2(d) and 2(c) can reduce the entire circuit depth by commuting and parallelizing quantum gates in a collective manner. That is, the subcircuit $S_{p_m=2}$ or $S_{p_m=3}$ inside a blue or red solid line box in Fig. 4 can commute with the CNOT gate in column 17 or 21, respectively. In the following we formulate a uniform version of such circuit rewriting rules as Theorem 2.

Theorem 2. Uniform circuit rewriting rule. In an n-qubit quantum circuit, we use S_{p_m} to denote a subcircuit that consists of an alternating sequence of 2^{p_m-1}CNOT gates and 2^{p_m-1} –

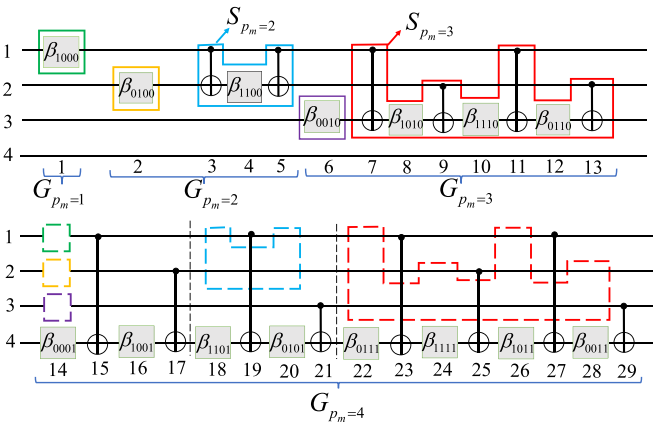

FIG. 4. Depth-optimization of the four-qubit circuit constructed from Theorem 1. When we move the subcircuits inside colored solid line boxes in $G_{p_m=1}$, $G_{p_m=2}$, and $G_{p_m=3}$ to the right to fill dashed vacant boxes of the same color in $G_{p_m=4}$, the overall circuit depth can be reduced from 24 to 16. This is an example of applying Theorem 2.

1 R_Z gates, where the control qubits of these CNOT gates targeted on qubit p_m are given in Eqs. (18) and (19), and all R_Z gates act on qubit p_m. Then S_{p_m} commutes with a $\text{CNOT}(p_m, n)$ gate for any integer $p_m \in [2, n-1]$, that is,

$$S_{p_m} \circ \text{CNOT}(p_m, n) = \text{CNOT}(p_m, n) \circ S_{p_m},$$

which is called a uniform circuit rewriting rule.

Proof. It can be seen from Eqs. (18) and (19) that each different CNOT control must appear an even number of times inside any S_{p_m}. Therefore, such a sequence S_{p_m} consisting of alternating CNOT and R_Z gates clearly commutes with a $\text{CNOT}(p_m, n)$ gate by alternately using the commutation rules in Figs. 2(a) and 2(b), where all additional CNOT gates would cancel out.

Based on Theorem 2, we can develop a depth-optimization procedure for reducing the depth of the n-qubit circuit from Theorem 1. By generalizing Fig. 4 to the circuit of any size n consisting of subcircuits $\{G_{p_m} : p_m = 1, 2, \ldots, n\}$, all 2^{p_m} gates in each $G_{1<p_m<n}$ can be divided into two subparts: (i) its leftmost R_Z gate and (ii) the rest 2^{p_m-1} CNOT and $2^{p_m-1}-1$ R_Z gates together denoted S_{p_m}. At first, the subpart S_{p_m} of $G_{p_m=n-1}$ can commute with all gates on the left of the leftmost $\text{CNOT}(n-1, n)$ gate in $G_{p_m=n}$ by noting Eq. (19), and then commute with this $\text{CNOT}(n-1, n)$ gate according to Theorem 2 to exactly fill vacancies on its right. Next, the subpart (i) of $G_{p_m=n-1}$ as a single R_Z gate can be moved to the vacant position at row $n-1$ and the first column of $G_{p_m=n}$. Similarly, the subpart S_{p_m} of $G_{p_m=n-2}$ can be moved to the right and filled the vacancies on the right of the leftmost $\text{CNOT}(n-2, n)$ gate of $G_{p_m=n}$ according to Theorem 2, and then the subpart (i) of $G_{p_m=n-2}$ as a single R_Z gate can be moved to the vacant position at row $n-2$ and the first column of $G_{p_m=n}$. In this way, all these subcircuits G_{p_m} with $p_m = n-1, n-2, \ldots, 3, 2$ can be regularly moved and embedded into corresponding vacancies of $G_{p_m=n}$ one after another, and at last $G_{p_m=1}$ as a single R_Z gate can be moved to the position at row 1 and the first column of $G_{p_m=n}$. As a final result, the depth of such an obtained n-qubit circuit is equal to that of $G_{p_m=n}$, that is, 2^n, which nearly halves the circuit depth $2^{n+1}-3$ resulted from previous Welch's method [20].

At this point, one can construct a circuit by Theorem 1 and then use Theorem 2 for optimizing the circuit depth. More significantly, we find these two steps can be skillfully combined to give a new circuit synthesis algorithm that not only ensures the asymptotically optimal gate count, but also automatically achieves an optimized depth as introduced in the following.

Note the essence of using Theorem 2 to optimize the depth of a circuit from Theorem 1 is to move gates in its smaller subcircuits G_{p_m} with $p_m = 1, 2, \ldots, n-1$ into specific vacancies of the rightmost subcircuit $G_{p_m=n}$, indicating that the positions of all these gates in the final optimized circuit can actually be predetermined. Based on this crucial observation, here we present Algorithm 1 as the key contribution of this paper, which can directly identify-and-embed CNOT and R_Z gates in each $G_{p_m}(p_m = 1, 2, \ldots, n)$ for piecing up the whole n-qubit circuit of depth 2^n. Specifically, we initialize the desired circuit QC_D as a substrate consisting of n rows and 2^n columns of vacancies, and then identify and embed each $G_{p_m<n}$ consisting of a R_Z gate and a subpart $S_{p_m<n}$, followed by the final $G_{p_m=n}$.

To illustrate the working principle of Algorithm 1 in a more intuitive way, we demonstrate the four-qubit depth-optimized circuit synthesis for implementing a diagonal operator $D(\vec{\theta} = [\theta_{0000}, \ldots, \theta_{1111}])$ as an example depicted in Fig. 5 with a description as follows.

(1) In Fig. 5(a), we initialize the four-qubit circuit QC_D as a substrate consisting of 4 rows and 16 columns of vacancies, and calculate all rotation angles denoted $[\beta_{0001}, \ldots, \beta_{1111}]$ of 15 nontrivial R_Z gates from the given $[\theta_{0000}, \ldots, \theta_{1111}]$. We also initialize the CNOT gate control set as $\lambda \leftarrow [0]$ and the one-bit Gray code sequence $GC_2 \leftarrow \{0, 1\}$ according to Eqs. (17a).

(2) In Fig. 5(b), we embed three R_Z gates denoted $R_Z(-\beta_{1000})$, $R_Z(-\beta_{0100})$, $R_Z(-\beta_{0010})$ into row 1, 2, 3 and column 1 of QC_D as marked green, orange, purple, respectively. Note each such R_Z gate belongs to $G_{p_m=1,2,3}$, respectively.

(3) In Fig. 5(c), we construct the subcircuit $S_{p_m=2} = \text{CNOT}(1,2) \circ R_Z(-\beta_{1100}; 2) \circ \text{CNOT}(1,2)$ by identifying all CNOT gate controls as $\lambda = [1, 1]$ and the angle parameter of the R_Z gate via GC_2, and then embed $S_{p_m=2}$ into columns 5-7 of QC_D with gates marked blue. Also, we generate the two-bit Gray code sequence $GC_4 = \{00, 10, 11, 01\}$.

(4) In Fig. 5(d), we construct the subcircuit $S_{p_m=3} = \text{CNOT}(1,3) \circ R_Z(-\beta_{1010}; 3) \circ \text{CNOT}(2,3) \circ R_Z(-\beta_{1110}; 3) \circ \text{CNOT}(1,3) \circ R_Z(-\beta_{0110}; 3) \circ \text{CNOT}(2,3)$ by identifying all CNOT gate controls as $\lambda = [1, 2, 1, 2]$ and angle parameters of three R_Z gates via GC_4, and then embed $S_{p_m=3}$ into columns 9-15 of QC_D with gates marked red. Also, we generate the three-bit Gray code sequence $GC_8 = \{000, 100, 110, 010, 011, 111, 101, 001\}$.

(5) Finally, in Fig. 5(e) we construct the subcircuit $G_{p_m=4} = R_Z(-\beta_{0001}; 4) \circ \text{CNOT}(1,4) \circ R_Z(-\beta_{1001}; 4) \circ \text{CNOT}(2,4) \circ R_Z(-\beta_{1101}; 4) \circ \text{CNOT}(1,4) \circ R_Z(-\beta_{0101}; 4) \circ \text{CNOT}(3,4) \circ R_Z(-\beta_{0111}; 4) \circ \text{CNOT}(1,4) \circ R_Z(-\beta_{1111}; 4) \circ \text{CNOT}(2,4) \circ R_Z(-\beta_{1011}; 4) \circ \text{CNOT}(1,4) \circ R_Z(-\beta_{0011}; 4) \circ \text{CNOT}(3,4)$ by identifying all CNOT gate

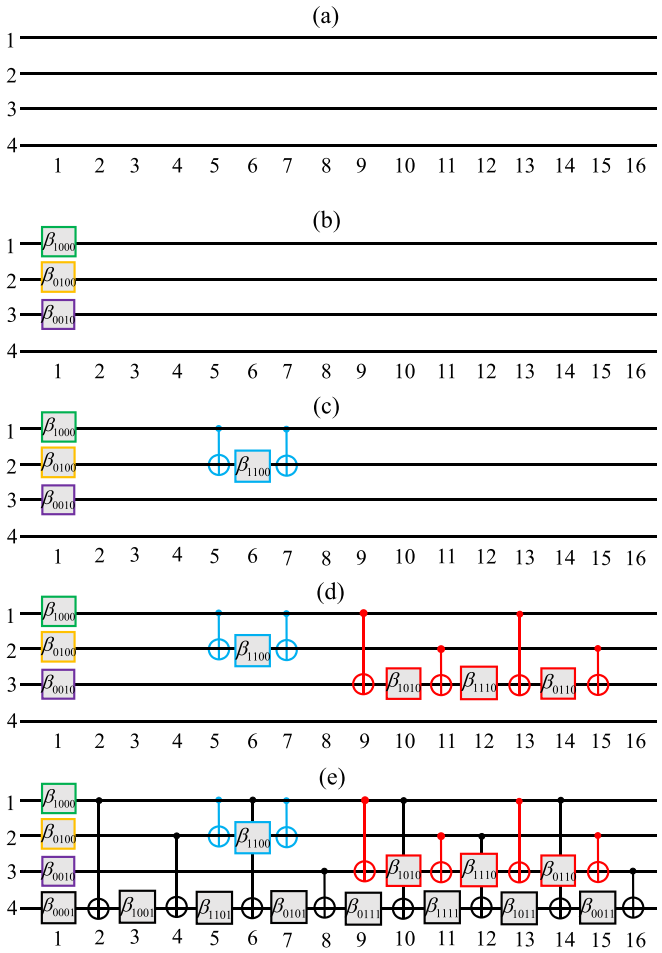

FIG. 5. Four-qubit depth-optimized circuit synthesis as an example to demonstrate Algorithm 1. In (a) we initialize the circuit as a substrate consisting of 4 rows and 16 columns of vacancies, and then successively identify and embed three R_Z gates marked green, orange, and purple, $S_{p_m} = 2$ with three gates marked blue, $S_{p_m} = 3$ with seven gates marked red, and $G_{p_m=4}$ with 16 gates marked black to achieve (b), (c), (d), and the final desired circuit QC_D in (e).

controls as $\lambda = [1, 2, 1, 3, 1, 2, 1, 3]$ and angle parameters of eight R_Z gates via GC_8, and then embed $G_{p_m=4}$ into columns 1 to 16 of QC_D with gates marked black. As a result, this circuit in Fig. 5(e) can realize any diagonal unitary matrix of size 16×16.

Similar to above example with $n = 4$, we can use Algorithm 1 to synthesize a {CNOT, R_Z} circuit of depth at most 2^n to realize any diagonal unitary operator given in Eq. (4). Since the depth of the circuit constructed by Welch's method [20] is $2^{n+1} - 3$, our generated circuit can achieve a nearly 50% depth reduction for the general case when all angle parameters of R_Z gates are nonzero.

D. Discussion on further optimization

As mentioned in Sec. II C, a circuit synthesis algorithm can have different performances on cases with different structures. For a more comprehensive study, here we have some discussions of possible further gate-count and depth optimization in terms of special cases besides the general case. Although

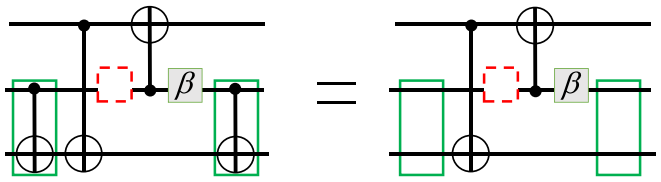

FIG. 6. Simplification techniques for canceling two CNOT gates in green boxes. The dashed red box generally indicates any subcircuit that commutes with the CNOT gate in green box.

the circuits obtained in Algorithm 1 hold for realizing general $D(\vec{\theta})$ with the asymptotically optimal gate count, it is worth noting that the number of required gates for implementing specific matrices may be further reduced. For example, if $D(\vec{\theta})$ is given by $\vec{\theta} = [0, 0, 0, 0, 0, 0, \pi, \pi]$, then the four R_Z gates in columns 1, 3, 5, 7 of the synthesized circuit in Fig. 3(c) have rotation angle values $\beta_{001} = \beta_{101} = \beta_{111} = \beta_{011} = 0$ and thus can be removed as identity matrices. Accordingly, the four CNOT gates in columns 2, 4, 6, 8 can be canceled by noting Fig. 2(c). In fact, a variety of commutation and rewriting rules related to the gate set {CNOT, R_Z} have been introduced for quantum circuit synthesis and optimization [20,27]. Considering the structure of our circuits synthesized from Algorithm 1, here we suppose a simple procedure that first removes all R_Z gates with angle parameters $\beta = 0$ and then implements the CNOT gate cancellation in Fig. 2(a) and Fig. 6 is usually effective for further reducing the gate count as well as circuit depth. Later, we will show how to apply the combination of our Algorithm 1 and optimization techniques described here to a practical use case in Sec. IV B.

IV. PERFORMANCE EVALUATION

In Sec. III C we theoretically revealed the circuit synthesized from Algorithm 1 can exhibit a depth reduction over the previous result. To evaluate the practical performance of our depth-optimized circuit synthesis algorithm, in this section we apply Algorithm 1 to a general case (the random diagonal operator) as well as a specific use case (the QAOA circuit).

A. Random diagonal unitary operators

In principle, our Algorithm 1 can generate a quantum circuit for implementing any give diagonal unitary matrix. Without loss of generality, we investigate the synthesis of n-qubit random diagonal matrices $D(\vec{\theta})$ such that 2^n angle parameters of $\vec{\theta}$ are uniformly distributed random variables in the interval $(0, 2\pi)$. In particular, such random diagonal unitaries may have an application in a quantum informational task called unitary 2-designs [31]. Specifically, we perform Algorithm 1 aimed at 300 random diagonal matrices $D(\vec{\theta})$ and obtain target {CNOT, R_Z} circuits with an average depth $d_1(n)$ for $2 \leqslant n \leqslant 16$ as shown in Table I. For comparison, we also employ Welch's method [20] to construct n-qubit {CNOT, R_Z} circuits with the average depth denoted $d_2(n)$ as recorded in Table I. As a result, the red curve in Fig. 7 shows that our circuits achieve substantial reductions in circuit depth compared with Welch's method [that is, $1 - d_1(n)/d_2(n)$] from 20% to 49.999% as n increases from 2 to 16.

TABLE I. Performance of our Algorithm 1 and Welch's method [20] to synthesize circuits aimed at implementing 300 n-qubit random diagonal unitary operators with $2 \leqslant n \leqslant 16$, where the average circuit depths are denoted as d_1 and d_2, respectively.

n	2	3	4	5	6	7	8	9	10	11	12	13	14	15	16
d_1	4	8	16	32	64	128	256	512	1024	2048	4096	8192	16 384	32 768	65 536
d_2	5	13	29	61	125	253	509	1021	2045	4093	8189	16 381	32 765	65 533	131 069

B. QAOA circuits on complete graphs

Quantum approximate optimization algorithm (QAOA) is one of the most promising quantum algorithms in the noisy intermediate-scale quantum (NISQ) era [32,33], which is suited for solving combinatorial optimization problems. Here we investigate the n-qubit QAOA circuit that generates QAOA ansatz state for MaxCut problem on an n-node complete graph as introduced in Ref. [17], where the internal part QC_D, sandwiched between Hadamard and R_X gates, consists of a series of $(n^2-n)/2$ subcircuits denoted

$$SC(\gamma; c, t) = \text{CNOT}(c, t) \circ R_Z(-2\gamma; t) \circ \text{CNOT}(c, t), \quad (20)$$

each of which acts on qubits c and t with $1 \leqslant c < t \leqslant n$ and can transform the basis state $|k\rangle$ as

$$|k\rangle = |k_1\rangle \ldots |k_c\rangle \ldots |k_t\rangle \ldots |k_n\rangle \to e^{i(-1)^{k_c \oplus k_t}\gamma}|k\rangle. \quad (21)$$

As a whole, the main subcircuit of QAOA is

$$\begin{aligned} QC_D(\gamma) = {} & SC(\gamma; 1, 2) \circ SC(\gamma; 1, 3) \circ \cdots \circ SC(\gamma; 1, n) \circ \\ & \times SC(\gamma; 2, n) \circ SC(\gamma; 2, n-1) \\ & \times \cdots \circ SC(\gamma; n-1, n), \end{aligned} \quad (22)$$

which can realize a diagonal matrix $D(\gamma)$ as

$$D(\gamma) = \sum_{k \in \{0,1\}^n} e^{i\theta_k}|k\rangle\langle k| \quad (23)$$

with the angle parameter

$$\theta_k = \gamma \sum_{1 \leqslant c < t \leqslant n} (-1)^{k_c \oplus k_t} \quad (24)$$

by using Eq. (21).

It can be seen that the circuit $QC_D(\gamma)$ in Eq. (22) has totally (n^2-n) CNOT gates, $(n^2-n)/2$ $R_Z(-2\gamma)$ gates, and depth $3(n^2-n)/2$ as exemplified by Fig. 8(a) for $n = 4$ [17], and we aim at the resynthesis of this important building block in QAOA circuits for achieving an optimized depth. For the original QAOA circuit with $QC_D(\gamma)$, the positions of all CNOT and $R_Z(-2\gamma)$ gates are fixed while the parameter γ is updated in each loop during running the QAOA. Accordingly, here for each size n we consider performing experiments on resynthesizing 100 circuit instances $QC_D(\gamma)$ with their parameter value γ varying over $(0, \pi)$.

For each target circuit determined by n and γ, we first use Eq. (24) to calculate all 2^n angle parameters denoted $\{\theta_k : k \in \{0,1\}^n\}$ of the diagonal unitary matrix $D(\gamma)$ represented by the circuit $QC_D(\gamma)$. Then we perform our Algorithm 1 to synthesize circuits for realizing each $D(\gamma)$, followed by the suitable optimization procedures introduced in Sec. III D. An example of our result with $n = 4$ is shown in Figs. 8(b) and 8(c), such that we obtain a circuit with a shorter depth of 12

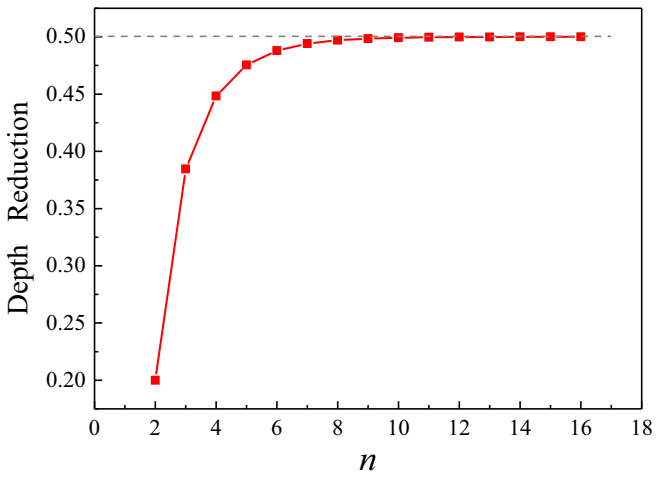

FIG. 7. Depth reduction by comparing the circuits synthesized from our Algorithm 1 with Welch's method [20] for implementing random diagonal unitary operators, which is calculated from Table I as $1 - d_1/d_2$ and approaches nearly 50% as the system size n increases to 16 qubits.

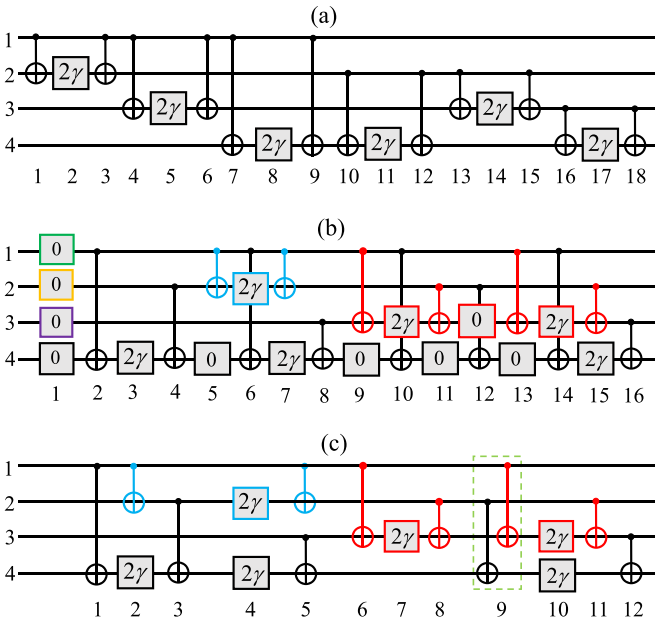

FIG. 8. Quantum circuit of depth 18 in (a) is an example of Eq. (22) to implement the diagonal operator inside a four-qubit QAOA circuit [17], which can be resynthesizd by our Algorithm 1 as shown in (b) and further optimized into a new one with 6 R_Z gates, 11 CNOT gates and depth 12 as shown in (c).

TABLE II. For implementing the diagonal operator in Eq. (23) of the n-qubit QAOA circuits with $3 \leqslant n \leqslant 14$, d_0 and d_1 represent the depth of original circuits in Eq. (22) and our final resynthesized circuits, respectively.

n	3	4	5	6	7	8	9	10	11	12	13	14
d_0	9	18	30	45	63	84	108	135	165	198	234	273
d_1	6	12	21	33	48	66	87	111	138	168	201	237

compared to the original circuit of depth 18 in Fig. 8(a). For the size $3 \leqslant n \leqslant 14$, the depths of original circuits in Eq. (22) denoted d_0 and our constructed circuits denoted d_1 are reported in Table II. The result presented in Fig. 9 reveals that our strategy can achieve a depth reduction over the original circuit (that is, $1 - d_1/d_0$) ranging from 13.19% to 33.33% with an average value of 22.05%.

Moreover, our synthesized $\{\text{CNOT}, R_Z(-\beta)\}$ circuits are shown to have the same configurations with $\beta = 2\gamma$ when we vary the input parameter value γ in Eq. (22), as exemplified by Fig. 8(c). Therefore, in this way we actually provide a functionally equivalent but depth-optimized ansatz circuit to implement the diagonal operator in such QAOA circuits instead of Eq. (22).

V. CONCLUSION

In this paper, we focus on the synthesis of quantum circuits over the gate set $\{\text{CNOT}, R_Z\}$ for implementing diagonal unitary matrices with both asymptotically optimal gate count and an optimized circuit depth, and conduct our study in a step-by-step way. First, we derive a kind of $\{\text{CNOT}, R_Z\}$ circuit with a regular structure and the asymptotically optimal gate count for general cases (see Theorem 1). Next, we develop a depth optimization procedure based on the uniform circuit rewriting rule (see Theorem 2) that can change the gate order for significantly reducing the n-qubit circuit depth. Finally, we further propose a circuit synthesis algorithm denoted Algorithm 1 such that once a circuit with the asymptotically optimal gate count is generated, its circuit depth has already been nearly halved compared with that from the previous well-known method [20], which is the key contribution of this paper. For the reader's convenience, we present intuitive instances to illustrate the working principle of our main results, e.g., Fig. 4 for Theorem 2 and Fig. 5 for Algorithm 1. Furthermore, we demonstrate the performance of our synthesis algorithm on two cases, including a random diagonal operator with up to 16 qubits and a QAOA circuit with up to 14 qubits, which can both achieve noteworthy reductions in circuit depth and thus might be useful for other cases in quantum computing as well. In addition, the proposed circuit rewriting rule in Theorem 2 can act as a subroutine for optimizing other similar $\{\text{CNOT}, R_Z\}$ circuits, e.g., the dashed red box in Fig. 6 including a subcircuit S_{p_m} in Theorem 2 can lead to CNOT cancellation. We believe these easy-to-follow and flexible techniques in this paper can facilitate the development of design automation for quantum computing [34].

Some problems that are worthy of further study are raised here.

(1) A recent study declares that any n-qubit diagonal unitary matrix can be realized by a quantum circuit that has depth $O(2^n/n)$ and $2^{n+3} + O(n^2/\log n)$ gates [10]. As comparison, our constructed circuit has depth 2^n and only $2^{n+1} - 3$ gates. Whether there exists a $\{\text{CNOT}, R_Z\}$ circuit that has the gate count $2^{n+1} - 3$ and circuit depth $O(2^n/n)$ for implementing the n-qubit diagonal operator is a quite attractive issue.

(2) Our synthesis procedure may need to apply CNOT gates to all pairs of qubits, and thus is suitable for physical systems with all-to-all connectivity such as neutral atoms [35], trapped ions [36,37], or more general ones [38]. Considering the restrictions on other near-term quantum hardware (e.g., superconducting systems), how to implement diagonal unitary operators with respect to certain hardware constraints (e.g., limited qubit connectivity) is a more complicated issue. In future work, we will consider how to adapt our synthesis algorithm to produce circuits that obey the connectivity restrictions and then compare its performance with existing schemes for NISQ architectures [39,40].

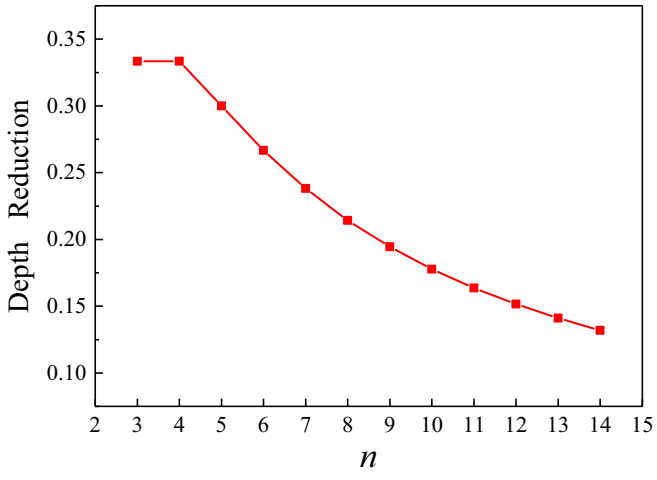

FIG. 9. Depth reduction by comparing the circuits resynthesized from our Algorithm 1 followed by simple optimizations in Sec. III D with the original circuits in Eq. (22) as an important part of QAOA circuits [17] for $3 \leqslant n \leqslant 14$, which is calculated from Table II as $1 - d_1/d_0$ and in the range of 13.19% to 33.33%.

ACKNOWLEDGMENTS

This work was supported by the National Natural Science Foundation of China (Grants No. 62102464, No. 62272492, and No. 61772565), the Guangdong Basic and Applied Basic Research Foundation (Grant No. 2020B1515020050), the Project funded by China Postdoctoral Science Foundation (Grants No. 2020M683049 and No. 2021T140761), and Guangdong Provincial Quantum Science Strategic Initiative (Grant No. GDZX2303007). We appreciate Dr. Li Zhang from South China Normal University for useful discussions.

[1] A. Barenco, C. H. Bennett, R. Cleve, D. P. DiVincenzo, N. Margolus, P. Shor, T. Sleator, J. A. Smolin, and H. Weinfurter, Elementary gates for quantum computation, Phys. Rev. A **52**, 3457 (1995).

[2] V. V. Shende, I. L. Markov, and S. S. Bullock, Minimal universal two-qubit controlled-not-based circuits, Phys. Rev. A **69**, 062321 (2004).

[3] M. Möttönen, J. J. Vartiainen, V. Bergholm, and M. M. Salomaa, Quantum circuits for general multiqubit gates, Phys. Rev. Lett. **93**, 130502 (2004).

[4] J. J. Vartiainen, M. Möttönen, and M. M. Salomaa, Efficient decomposition of quantum gates, Phys. Rev. Lett. **92**, 177902 (2004).

[5] V. Bergholm, J. J. Vartiainen, M. Möttönen, and M. M. Salomaa, Quantum circuits with uniformly controlled one-qubit gates, Phys. Rev. A **71**, 052330 (2005).

[6] V. V. Shende, S. S. Bullock, and I. L. Markov, Synthesis of quantum logic circuits, in *Proceedings of the 2005 Asia and South Pacific Design Automation Conference*, ASP-DAC '05 (Association for Computing Machinery, New York, 2005), pp. 272–275.

[7] M. Amy, D. Maslov, M. Mosca, and M. Roetteler, A meet-in-the-middle algorithm for fast synthesis of depth-optimal quantum circuits, IEEE Trans. Comput.-Aided Des. Integr. Circuits Syst. **32**, 818 (2013).

[8] M. Saeedi and I. L. Markov, Synthesis and optimization of reversible circuits—a survey, ACM Computing Surveys (CSUR) **45**, 1 (2013).

[9] O. D. Matteo and M. Mosca, Parallelizing quantum circuit synthesis, Quantum Sci. Technol. **1**, 015003 (2016).

[10] X. Sun, G. Tian, S. Yang, P. Yuan, and S. Zhang, Asymptotically optimal circuit depth for quantum state preparation and general unitary synthesis, IEEE Transactions on Computer-Aided Design of Integrated Circuits and Systems **42**, 3301 (2023).

[11] S. Zhang, J. Wu, and L. Li, Characterization, synthesis, and optimization of quantum circuits over multiple-control Z-rotation gates: A systematic study, Phys. Rev. A **108**, 022603 (2023).

[12] Y. Nakata and M. Murao, Diagonal quantum circuits: Their computational power and applications, Eur. Phys. J. Plus **129**, 152 (2014).

[13] M. A. Nielsen and I. L. Chuang, *Quantum Computation and Quantum Information: 10th Anniversary Edition* (Cambridge University Press, Cambridge, England, 2010).

[14] G.-L. Long, Grover algorithm with zero theoretical failure rate, Phys. Rev. A **64**, 022307 (2001).

[15] F. Toyama, W. Van Dijk, and Y. Nogami, Quantum search with certainty based on modified grover algorithms: Optimum choice of parameters, Quantum Info. Proc. **12**, 1897 (2013).

[16] M. Alam, A. Ash-Saki, and S. Ghosh, An efficient circuit compilation flow for quantum approximate optimization algorithm, in *57th ACM/IEEE Design Automation Conference* (ACM, New York, 2020), pp. 1–6.

[17] D. Lykov and Y. Alexeev, Importance of diagonal gates in tensor network simulations, in *2021 IEEE Computer Society Annual Symposium on VLSI (ISVLSI)* (IEEE, New York, 2021), pp. 447–452.

[18] Y. Xu, S. Zhang, and L. Li, Quantum algorithm for learning secret strings and its experimental demonstration, Physica A **609**, 128372 (2022).

[19] L. Li, J. Luo, and Y. Xu, Winning mastermind overwhelmingly on quantum computers, arXiv:2207.09356.

[20] J. Welch, D. Greenbaum, S. Mostame, and A. Aspuru-Guzik, Efficient quantum circuits for diagonal unitaries without ancillas, New J. Phys. **16**, 033040 (2014).

[21] I. Kassal, S. P. Jordan, P. J. Love, M. Mohseni, and A. Aspuru-Guzik, Polynomial-time quantum algorithm for the simulation of chemical dynamics, Proc. Natl. Acad. Sci. **105**, 18681 (2008).

[22] M. S. Alam, S. Hadfield, H. Lamm, and A. C. Y. Li (SQMS Collaboration), Primitive quantum gates for dihedral gauge theories, Phys. Rev. D **105**, 114501 (2022).

[23] Y. Nakata, M. Koashi, and M. Murao, Generating a state t-design by diagonal quantum circuits, New J. Phys. **16**, 053043 (2014).

[24] F. Leymann and J. Barzen, The bitter truth about gate-based quantum algorithms in the NISQ era, Quantum Sci. Technol. **5**, 044007 (2020).

[25] S. S. Bullock and I. L. Markov, Asymptotically optimal circuits for arbitrary n-qubit diagonal computations, Quantum Inf. Comput. **4**, 27 (2004).

[26] S. Bravyi, D. Gosset, and R. König, Quantum advantage with shallow circuits, Science **362**, 308 (2018).

[27] Y. Nam, N. J. Ross, Y. Su, A. M. Childs, and D. Maslov, Automated optimization of large quantum circuits with continuous parameters, npj Quantum Inf. **4**, 23 (2018).

[28] N. Abdessaied and R. Drechsler, in *Reversible and Quantum Circuits: Optimization and Complexity Analysis* (Springer, Berlin, 2016), Chap. 2, p. 35.

[29] F. Gray, Pulse code communication, United States Patent Number 2632058 (1953).

[30] J. R. Bitner, G. Ehrlich, and E. M. Reingold, Efficient generation of the binary reflected gray code and its applications, Communications of the ACM **19**, 517 (1976).

[31] Y. Nakata, C. Hirche, C. Morgan, and A. Winter, Unitary 2-designs from random X- and Z-diagonal unitaries, J. Math. Phys. **58**, 052203 (2017).

[32] E. Farhi, J. Goldstone, and S. Gutmann, A quantum approximate optimization algorithm, arXiv:1411.4028.

[33] K. Bharti, A. Cervera-Lierta, T. H. Kyaw, T. Haug, S. Alperin-Lea, A. Anand, M. Degroote, H. Heimonen, J. S. Kottmann, T. Menke, W.-K. Mok, S. Sim, L.-C. Kwek, and A. Aspuru-Guzik, Noisy intermediate-scale quantum algorithms, Rev. Mod. Phys. **94**, 015004 (2022).

[34] A. Zulehner and R. Wille, *Introducing Design Automation for Quantum Computing* (Springer, New York, 2020).

[35] D. Bluvstein, H. Levine, G. Semeghini, T. T. Wang, S. Ebadi, M. Kalinowski, A. Keesling, N. Maskara, H. Pichler, M. Greiner, V. Vuletić, and M. D. Lukin, A quantum processor based on coherent transport of entangled atom arrays, Nature (London) **604**, 451 (2022).

[36] C. Figgatt, A. Ostrander, N. M. Linke, K. A. Landsman, D. Zhu, D. Maslov, and C. Monroe, Parallel entangling operations on a universal ion-trap quantum computer, Nature (London) **572**, 368 (2019).

[37] K. A. Landsman, Y. Wu, P. H. Leung, D. Zhu, N. M. Linke, K. R. Brown, L. Duan, and C. Monroe, Two-qubit entangling

gates within arbitrarily long chains of trapped ions, Phys. Rev. A **100**, 022332 (2019).

[38] J. Ramette, J. Sinclair, Z. Vendeiro, A. Rudelis, M. Cetina, and V. Vuletić, Any-to-any connected cavity-mediated architecture for quantum computing with trapped ions or rydberg arrays, PRX Quantum **3**, 010344 (2022).

[39] B. Nash, V. Gheorghiu, and M. Mosca, Quantum circuit optimizations for nisq architectures, Quantum Sci. Technol. **5**, 025010 (2020).

[40] V. Vandaele, S. Martiel, and T. G. de Brugière, Phase polynomials synthesis algorithms for NISQ architectures and beyond, Quantum Sci. Technol. **7**, 045027 (2022).